Available online at www.sciencedirect.com
ScienceDirect
Chemical Physics Letters 437 (2007) 218–223
CHEMICAL PHYSICS LETTERS
www.elsevier.com/locate/cplett

A molecular dynamics study of the effect of a substrate on catalytic metal clusters in nucleation process of single-walled carbon nanotubes

Yasushi Shibuta [a,*], Shigeo Maruyama [b]

[a] Department of Materials Engineering, The University of Tokyo, 7-3-1 Hongo, Bunkyo-ku, Tokyo 113-8656, Japan
[b] Department of Mechanical Engineering, The University of Tokyo, 7-3-1 Hongo, Bunkyo-ku, Tokyo 113-8656, Japan

Received 18 December 2006; in final form 2 February 2007
Available online 12 February 2007

Abstract

The effect of the substrate on catalytic metal clusters in nucleation process of single-walled carbon nanotubes was studied by classical molecular dynamics (MD) simulation. The melting point of a nickel cluster increased with increasing catalyst–substrate interaction. During clustering process of carbon atoms via a nickel cluster on a substrate, a layered structure of fcc(1 1 1) was formed parallel to the substrate and a graphene was also generated parallel to the layer in case of strong catalyst–substrate interaction while the orientation of nickel cluster was not affected by the substrate in case of weak interaction.

1. Introduction

Developments of large-scale and high-purity generation technique for single-walled carbon nanotubes (SWNTs) [1] are desired for the practical applications of this fascinating new material. In addition to previously known laser furnace [2] and arc discharge technique [3], catalytic chemical vapor deposition (CCVD) methods [4] have been proposed for the possibility of large-scale production at low cost. This method falls into two type by the condition of metal catalyst: the floated catalyst and the supported-catalyst. The high-pressure carbon monoxide (HiPco) process [5] using a floated catalyst is one of the commercially feasible techniques for the mass production of SWNTs. However, they often suffer from the mixing of catalytic metal particles and amorphous carbon impurities among the produced SWNTs. On the other hand, Murakami et al. [6] developed high-purity product technique of vertical aligned SWNTs using the flat quartz substrate as a supporter, which is followed by the production technique, so-called 'super-growth' [7].

For the better condition in CCVD method, the role of the catalytic metals has been widely studied. Noda et al. [8] examined the best concentration ratio of Mo–Co binary metal nano-particle using combinatorial method. We have studied the graphitization ability of the transition metal cluster by classical molecular dynamics (MD) simulation [9]. However, the effect of the substrate on the catalytic ability is still unknown since there are many chemical reaction between the substrate and catalyst metals [10] during the CVD process at high temperature. For example, the role of oxygen functionality on the substrate surface is under discussion. Supposedly, substrates such as alumina or zeolite which have porous sites may work not only as supporting catalytic metals but also affecting dissociation of carbon-source molecules during formation process of SWNTs though substrates such as flat quartz or oxide-silicon surface does not affect it from experimental views. In this study, we assumed the substrate does not affect the dissociation process for the purpose of focusing on the effect of the substrate on the catalytic metal atoms.

* Corresponding author. Fax: +81 3 5841 8653.
E-mail address: shibuta@material.t.u-tokyo.ac.jp (Y. Shibuta).

0009-2614/$ - see front matter © 2007 Elsevier B.V. All rights reserved.
doi:10.1016/j.cplett.2007.02.019

The possibility of the dissociation process of carbon-source molecules via substrates must be considered in the next stage.

As a numerical approach, Ding et al. [11] examined the structure and thermal properties of supported iron cluster by classical MD simulation. They showed the strong cluster–substrate interaction increased melting temperature of the iron cluster on the substrate. One of us examined the interaction energy between graphene and metal catalyst cluster on the substrate [12]. In this Letter, the effect of the substrate on the catalytic metal cluster during the nucleation process was studied. Firstly, dependence of the cluster–substrate interaction on the structure of the nickel cluster and nickel-carbide cluster on the substrate was examined in Section 3. Next, nucleation process of nanotube caps from a nickel cluster on the substrate was calculated and the dependence of the substrate–catalyst interaction on the graphitic ability of the catalytic metal cluster was examined in Section 4.

2. Simulation methodology

A classical MD method was used to study the effect of a substrate on catalytic metal clusters during initial nucleation process of SWNTs. A Brenner potential [13] was used to describe a covalent bond between carbon atoms in the cluster. A many-body potential function [14] that was constructed for transition metal carbide cluster was used to describe a nickel–nickel and nickel–carbon bonds. Parameter sets of these potential functions are listed in Tables 1 and 2. A standard 6–12 Lennard-Jones potential, with the parameters $\varepsilon = 2.5$ meV and $\sigma = 3.37$ Å [15], was used to describe the intermolecular interaction between isolated carbon atoms in the gas phase.

In addition, the interaction between metal atoms in the cluster and the planar substrate was expressed using an one-dimensional averaged Lennard-Jones (1DLJ) potential [16]:

$$F(z) = D_e\left\{\frac{1}{5}\left(\frac{z}{\sigma}\right)^{-10} - \frac{1}{2}\left(\frac{z}{\sigma}\right)^{-4}\right\} \tag{1}$$

where z is the coordinate normal to the substrate plane. This potential function represents the integrated interaction between a metal atom in the cluster and all atoms on the substrate by a standard 6–12 Lennard-Jones potential function. The parameter σ is set to 3.23 Å, determined from the van der Waals radius of a Si atom [12]. The parameter D_e was varied from 0.5 to 1.25 eV at 0.25 eV intervals in order to describe the variable affinity of the metal cluster for the substrate.

The velocity Verlet method was used to integrate the classical equation of motion with a time step of 0.5 fs. A Berendsen thermostat [17] was used for temperature control with a relaxation time of 0.17 ps.

3. Dependence of cluster–substrate interaction on the structure of a metal cluster

Firstly, dependence of cluster–substrate interaction on the structure of a nickel cluster and a nickel-carbide cluster was examined in the following way. A face-centered cubic (fcc) structure of Ni_{256} was annealed without substrate-support for 2 ns at 2000 K. For the initial structure of a nickel-carbide cluster, a nonstoichiometric cluster, $Ni_{256}C_{53}$ obtained from our previous simulation [15] for nucleation process of SWNTs from a floated nickel cluster was used. The clusters were then annealed on the substrate for 100 ps at 500 K. After that controlled temperature was increased from 500 K to 3500 K with the rate of 1 K per 1 ps. Various range of the binding energy of the 1DLJ potential was examined from 0.5 eV to 1.25 eV in 0.25 eV intervals.

The melting point of a cluster is defined as a temperature where Lindemann index becomes 0.1 [18]. The Lindemann index, δ is defined as the root mean squared (rms) bond-length fluctuation as follows:

$$\delta = \frac{2}{N(N-1)}\sum_{i<j}\frac{\sqrt{\langle r_{ij}^2\rangle - \langle r_{ij}\rangle^2}}{\langle r_{ij}\rangle} \tag{2}$$

where r_{ij} is the distance between atom i and j, and N is the number of atoms in the cluster. Melting points of the nickel clusters on the substrate of the binding energy, 0.25, 0.75 and 1.25 eV were defined as 2571, 2647 and 2720 K, respectively. Abrupt increase of the potential energy against temperature was observed at the defined melting point as shown in Fig. 1a. The melting point decreased with decreasing the catalyst–substrate interaction. This is consistent with the behavior predicted by Gibbs–Thomson's

Table 1
Potential parameters for nickel–nickel interactions

	S	β (1/Å)	D_{e1} (eV)	D_{e2} (eV)	C_D	R_{e1} (Å)	R_{e2} (Å)	C_R	R_1 (Å)	R_2 (Å)
Ni–Ni [14]	1.3	1.55	0.74	1.423	0.365	2.520	0.304	0.200	2.7	3.2

Table 2
Potential parameters for carbon–carbon and carbon–nickel interactions

	D_e (eV)	S	β (1/Å)	R_e (Å)	R_1 (Å)	R_2 (Å)	b	δ	a_0	c_0	d_0
C–C [13]	6.325	1.29	1.5	1.315	1.7	2.0	–	0.80409	0.011304	19	2.5
Ni–C [14]	2.4673	1.3	1.8706	1.7628	2.7	3.0	0.0688	−0.5351	–	–	–

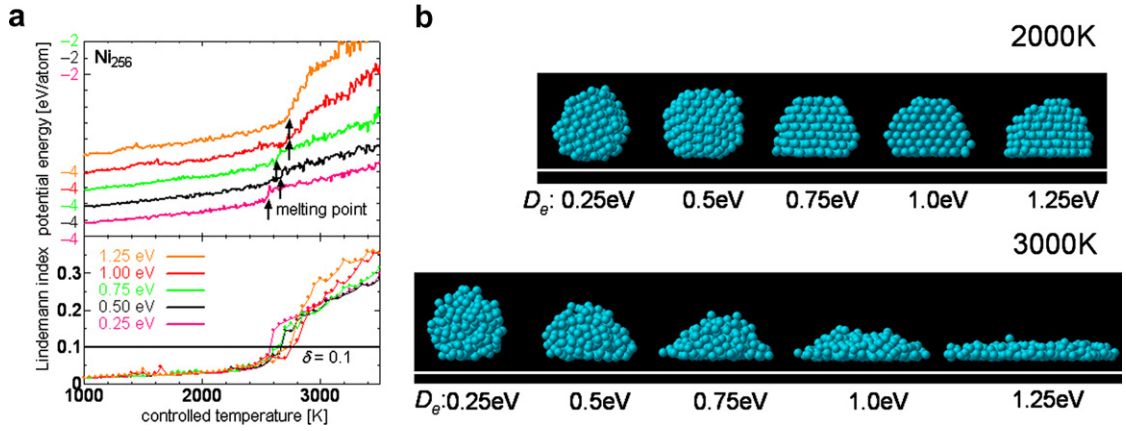

Fig. 1. (a) The potential energy of Ni_{256} per atom and the Lindemann index against controlled temperature. The melting point is defined as the temperature where the Lindemann index is 0.1. At melting temperature, the potential energy abruptly increases shown by the black arrows. The data was displaced to the y-axis for clarity. (b) Annealed structure of the nickel clusters on a substrate of various interaction energies at 2000 K and 3000 K. The clusters changed to liquid droplets and wetted to the substrate more strongly as increasing the catalyst–substrate interaction energy at 3000 K.

equation; depression of the melting temperature is proportional to the interfacial curvature. That is, the volume of a droplet on a substrate, V is expressed as follows:

$$V = \pi r^3 \frac{(1-\cos\theta)^2(2+\cos\theta)}{3} \tag{3}$$

The radius, r decreases with increasing the contact angle, θ when the volume is constant and the contact angle increase with decreasing the catalyst–substrate interaction as shown in Fig. 1b. The radius decreases (i.e. the interfacial curvature increases) with decreasing the catalyst–substrate interaction. Hence, melting point decreased with decreasing the catalyst–substrate interaction. The value of the melting point is sensitive to the potential parameter. Hence, the quantitative discussion about melting point is not shown in this Letter. Further discussion for dependence of potential parameters on the melting point will be needed in the next stage.

Below the melting point by the many-body potential function we have constructed, potential energy per atom was proportional to the controlled temperature; the gradient is 0.14 eV K^{-1} independent of the cluster–substrate interaction energy. However, the temperature range of the abrupt change increased with increasing the catalyst–substrate interaction energy. In case of the 0.25 eV as the binding energy of 1DLJ potential, the range of the abrupt increase was less than 100 K though it was more than 200 K in case of the binding energy of 1.25 eV.

The snapshots of the structure of nickel clusters on a substrate at 2000 K and 3000 K were shown in Fig. 1b. Below the melting point defined above, the clusters kept its crystal structure and had the facet surface. Island structure was kept even on the substrate of the strong catalyst–substrate interaction. However, the nickel clusters changed to liquid droplets at 3000 K. The clusters wetted to the substrate more strongly with increasing the catalyst–substrate interaction energy. The spherical structure disappeared and the metal atoms wetted completely on the substrate forming a layer structure in case of 1.25 eV as the binding energy of 1DLJ potential.

On the other hand, the abrupt increase of the potential energy of the nickel atoms in the nickel-carbide cluster was not observed as shown in Fig. 2a. The potential energy of the nickel atoms on the substrate of the binding energy, 0.5 eV decreased from −3.7 eV to −5.25 eV at 2000 K because of the additional nickel–carbon bonding. Gradient of the potential energy against controlled temperature increased continuously. The Lindemann indices for nickel–nickel and carbon–carbon bonds in the nickel-carbide cluster were shown in Fig. 2b. The Lindemann indices did not increased rapidly compared with that of the nickel cluster as in the case of the potential energy. The melting temperature of the nickel-carbide clusters were estimated between 2500 K and 2600 K by the indices of the nickel–nickel bonds. Oh the other hand, the Lindemann index for carbon–carbon increased with increasing temperature across the value of 0.1 around 3000 K. However, the potential energy of the carbon atoms in the nickel-carbide cluster decreased as increasing the controlled temperature. This shows carbon atoms diffused to the more stable position with increasing temperature.

The snapshots of the structure of the nickel-carbide cluster on the substrate at 2000 K and 3000 K were shown in Fig. 2c. The nickel atoms did not take the crystal structure at 2000 K. However, the clusters kept island structure even at the strong catalyst-interaction energy because the nickel–carbon bonding decreased the potential energy of the cluster about 1.55 eV per nickel atom compared with that of the nickel cluster at 2000 K as described above. The abrupt increase of potential energy of the nickel cluster was caused by structure change from crystal structure to disorder. On the other hand, the nickel carbide cluster took the disorder structure below the melting point. Hence, the abrupt increase of potential energy was not observed in Fig. 2a. The nickel-carbide cluster wetted to the substrate with increasing the catalyst–substrate interaction in

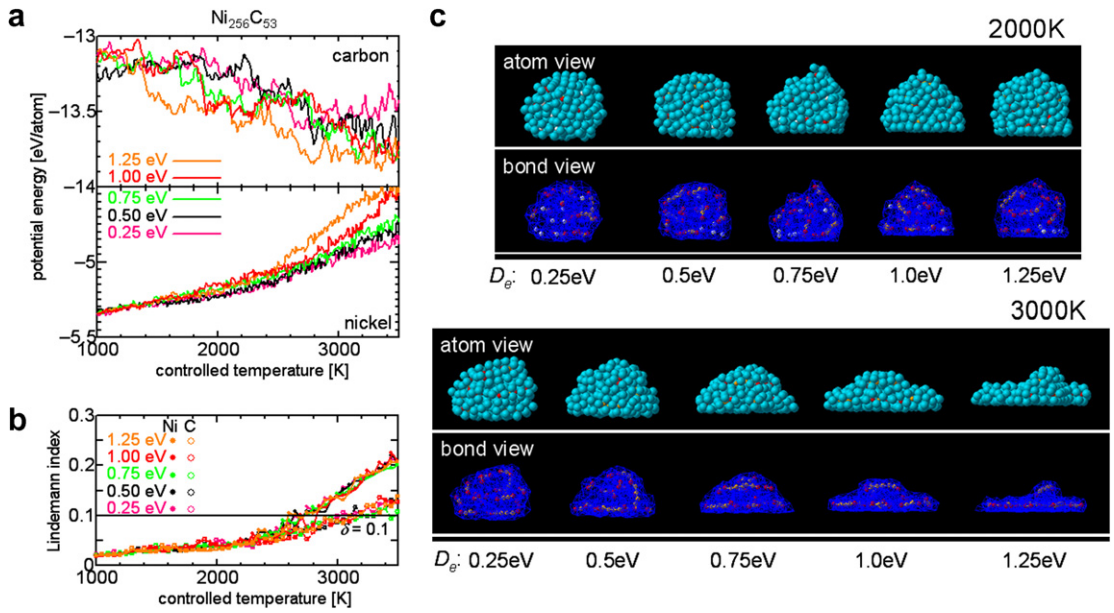

Fig. 2. (a) The potential energy per atom of a nonstoichiometric nickel-carbide cluster ($Ni_{256}C_{53}$) against controlled temperature. The abrupt change was not observed. The potential energy of the carbon atom in the cluster decreased as increasing temperature. (b) The Lindemann indices for nickel–nickel and carbon–carbon bonds in the nickel-carbide cluster against controlled temperature. (c) Annealed structure of the nickel-carbide cluster on a substrate of various interaction energies at 2000 K and 3000 K. In the bond view, nickel atoms are not shown for clarity. The layer structure was observed with the strong interaction energy at 3000 K. Carbon atoms were distributed at interlayer region.

3000 K as in the case of the nickel cluster. The layered structure was observed in case of the binding energy of 1DLJ potential, 1.25 eV. Carbon atoms were distributed at interlayer region.

4. Molecular dynamics simulation of clustering process of carbon atoms

Next, nucleation process of nanotube caps from a nickel cluster on the substrate was examined. One of the equilibrated nickel clusters obtained in Section 3 with the binding energy of 0.25, 0.5 and 1.0 eV at 2000 K were placed on the bottom of a cubic cell of $(20\ \text{nm})^3$, respectively. Then, five hundreds of isolated carbon atoms were randomly allocated in a cell as shown in Fig. 3. The top and bottom boundaries had mirror boundary condition and others had periodical boundary conditions. The controlled temperature was set to 2500 K. The density of isolated carbon atoms was kept constant by adding a new carbon atom at a random place in the cell whenever a carbon atom attached to the nickel cluster.

Fig. 4 shows the snapshots of clustering process of carbon atoms via a nickel cluster on the substrate. As increasing the binding energy, a layered structure of fcc(1 1 1) was formed parallel to the substrate and a graphene was generated parallel to the layer. Views from bottom show the nickel atoms on the 2D closed-packed facet and the graphene has geometrical match. In our previous report, the 2D closed-packed facet of the transition metal atoms can be a template of the graphene from both geometrical and energetic standpoint [9]. Hence, the orientation of the 2D

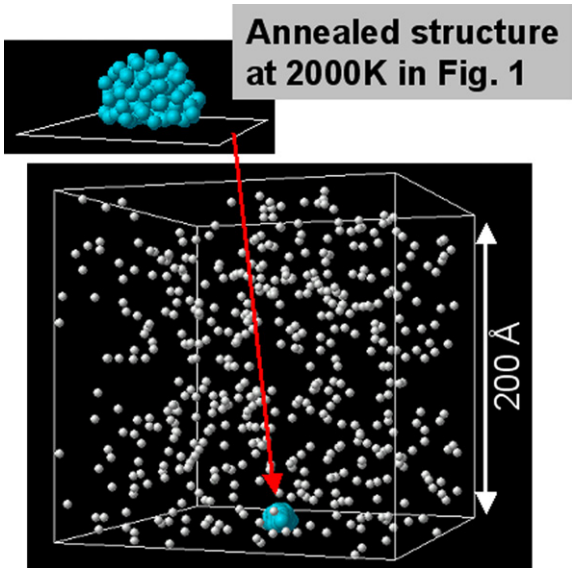

Fig. 3. An initial condition for the clustering process. Five hundreds of isolated carbon atoms were randomly allocated in a 20 nm cubic cell. One of the equilibrated nickel clusters obtained in Fig. 1 were placed on the bottom of the cell.

closed-packed facet is a key to determine the direction to which a graphene separate from a catalytic cluster.

In case of the strong cluster–substrate interaction, the 2D closed-packed facet was formed parallel to the substrate and the graphene also separated from the edge of the cluster parallel to the substrate. It is difficult to form the cap structure in that condition. On the other hand,

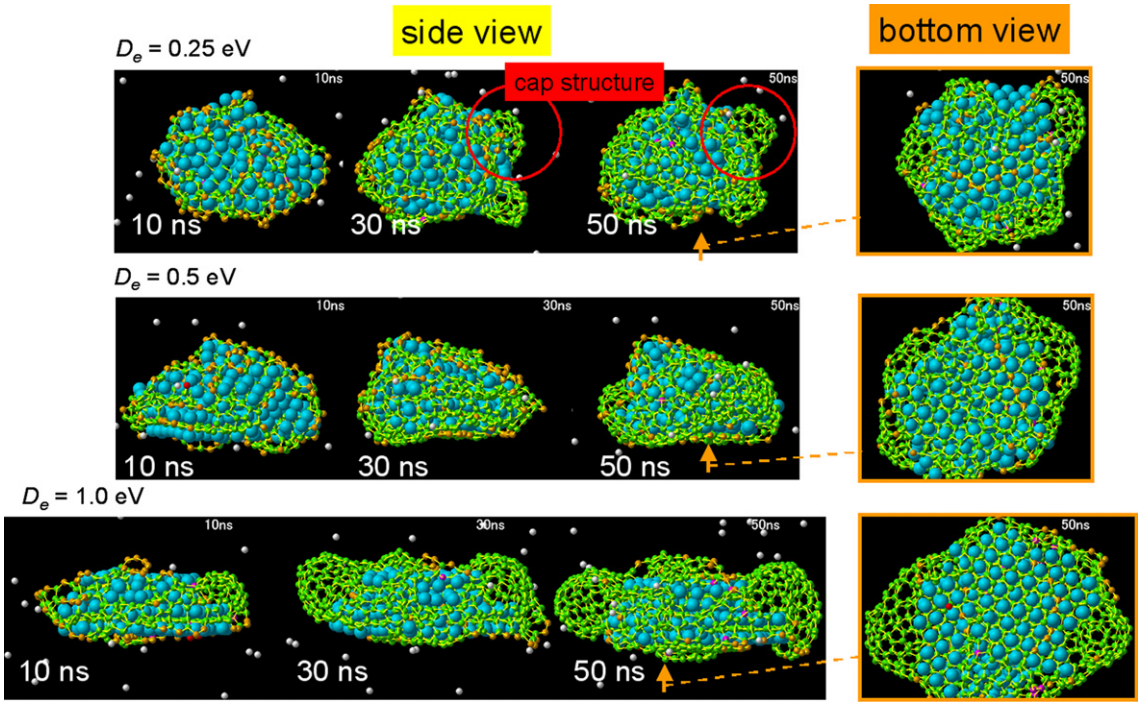

Fig. 4. Snapshots of clustering process of carbon atoms via a nickel cluster on a substrate with the binding energy of 0.25, 0.5 and 1 eV. The white, red, orange, green and purple ball represent carbon atom that has 0, 1, 2, 3 and 4 carbon-covalent bonds, respectively. Views from bottom show the nickel atoms on the 2D closed-packed facet and the graphene has geometrical match. The cap structure was observed at the hump of the cluster on the substrate of binding energy 0.25 eV. (For interpretation of the references in colour in this figure legend, the reader is referred to the web version of this article.)

the orientation was not affected by the substrate in case of weak cluster–substrate interaction. Hence, the graphene separated from the cluster independent of the direction of the substrate. Some of them were separated around a facet at a hump of the cluster and formed the cap structure. The formation process of the cap structure was similar to our previous study of nucleation process of SWNTs from the floated Ni_{256} [15]. That is, after saturation of carbon atoms into the nickel cluster, hexagonal carbon networks were formed inside the cluster and separated around a facet at the hump of the cluster and formed the cap structure.

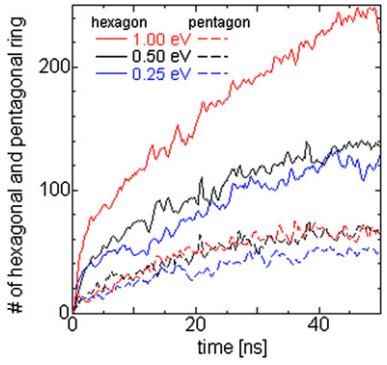

Fig. 5. Time series of the number of hexagonal and pentagonal rings in the catalytic metal cluster in the 50 ns calculation of the clustering process. The cluster on the strong catalyst–substrate interaction made more hexagonal ring than it on the weak interaction.

Fig. 5 shows time series of the number of hexagonal and pentagonal rings in the nickel clusters during clustering process. The number of the hexagonal rings in the cluster on the substrate of strong catalyst–substrate interaction (1.0 eV) increased about twice as fast as in the cluster on the substrate of weak interaction (0.25 eV). It is because the nickel cluster wets more strongly and the fcc(1 1 1) facet was formed parallel to the substrate under the strong interaction energy. The facet has geometrical match with graphene. Hence, the graphene is generated parallel to the substrate easily as if the 2D closed-packed facet were a template. However, the suitable hump did not exist on the cluster on the strong catalyst–cluster interaction. Cap structure was not nucleated though the large graphene surface was generated. Other than the graphitization ability, the structure of the catalyst cluster itself may be important.

5. Conclusion

The effect of the substrate on catalytic metal atoms in nucleation process of SWNTs was studied. Firstly, dependence of a cluster–substrate interaction on the structure of a nickel cluster and a nickel-carbide cluster was examined. The melting point of a cluster was defined as a temperature using Lindemann index. Abrupt increases of the potential energy were observed at the defined melting temperature with increasing temperature in case of the nickel cluster. It was caused by the structure change from crystal to disorder. The melting point decreased with decreasing

the catalyst–substrate interaction. Addition of carbon atoms in the nickel cluster made the cluster disorder below the melting point resulting in continuous increase of the potential energy.

Next, nucleation process of nanotube caps from nickel cluster on a substrate was analyzed. In case of the strong cluster–substrate interaction, a layered structure was observed with fcc(1 1 1) facet parallel to the substrate and a graphene was generated parallel to the substrate. From the cluster on the weak interaction, on the other hand, the orientation was not affected by the substrate. Then, the graphene separated from the cluster independent of the direction of the substrate. Some of them were separated around a facet at a hump of the cluster and formed the cap structure. Hence, for the better condition for the nucleation of cap structure of SWNT, not only the graphitization ability but also structure of the catalyst cluster may be important.

Acknowledgements

Part of this work was financially supported by Grant-in-Aid for Young Scientists (a) (No. 18686017) from MEXT, Japan. Y.S. thanks Prof. Toshio Suzuki (Department of Materials Engineering, The University of Tokyo) for insightful discussions.

References

[1] S. Iijima, T. Ichihashi, Nature 363 (1993) 603.
[2] A. Thess et al., Science 273 (1996) 483.
[3] C. Journet et al., Nature 388 (1997) 756.
[4] H. Dai, A.G. Rinzler, P. Nikolaev, A. Thess, D.T. Colbert, R.E. Smalley, Chem. Phys. Lett. 260 (1996) 471.
[5] P. Nikolaev, M.J. Bronikowski, R.K. Bradley, F. Rohmund, D.T. Colbert, K.A. Smith, R.E. Smally, Chem. Phys. Lett. 313 (1999) 91.
[6] Y. Murakami, S. Chiashi, Y. Miyauchi, M. Hu, M. Ogura, T. Okubo, S. Maruyama, Chem. Phys. Lett. 385 (2004) 298.
[7] K. Hata, D.N. Futaba, K. Mizuno, T. Namai, M. Yumura, S. Iijima, Science 306 (2004) 1362.
[8] S. Noda, H. Sugime, T. Osawa, Y. Tsuji, S. Chiashi, Y. Murakami, S. Maruyama, Carbon 44 (2006) 1414.
[9] Y. Shibuta, S. Maruyama, Comput. Mater. Sci., doi:10.1016/j.commatsci.2006.10.007.
[10] M. Hu, Y. Murakami, M. Ogura, S. Maruyama, T. Okubo, J. Catal. 255 (2004) 230.
[11] F. Ding, K. Bolton, A. Rosen, Appl. Surf. Sci. 252 (2006) 5254.
[12] Y. Shibuta, J.A. Elliott, Chem. Phys. Lett. 427 (2006) 365.
[13] D.W. Brenner, Phys. Rev. B 42 (1990) 9458.
[14] Y. Yamaguchi, S. Maruyama, Euro. Phys. J. D 9 (1999) 385.
[15] Y. Shibuta, S. Maruyama, Chem. Phys. Lett. 382 (2003) 381.
[16] S. Maruyama, T. Kurashige, S. Matsumoto, Y. Yamaguchi, T. Kimura, Micro. Thermophys. Eng. 2 (1998) 42.
[17] H.J.C. Berendsen, J.P.M. Postma, W.F. van Gunsteren, A. DiNola, J.R. Haak, J. Chem. Phys. 81 (1984) 3684.
[18] S.K. Nayak, S.N. Khanna, B.K. Rao, P. Jena, J. Phys.: Condens. Matter 10 (1998) 10853.